Journal of Molecular Structure 1003 (2011) 129–133

Contents lists available at SciVerse ScienceDirect

Journal of Molecular Structure

journal homepage: www.elsevier.com/locate/molstruc

Crystal structure refinement, spectroscopic study and magnetic properties of yttrium hexacyanoferrate (III)

Diego M. Gil [a], M.C. Navarro [a], M.C. Lagarrigue [a], Julio Guimpel [b,1], Raúl E. Carbonio [c,1], M. Inés Gómez [a,*]

[a] Instituto de Química Inorgánica, Facultad de Bioquímica, Química y Farmacia, Universidad Nacional de Tucumán, Ayacucho 471, 4000 San Miguel de Tucumán, Argentina
[b] Centro Atómico Bariloche, Comisión Nacional de Energía Atómica and Instituto Balseiro, Universidad Nacional de Cuyo, Avda. Ezequiel Bustillo 9.500, 8400 San Carlos de Bariloche, Río Negro, Argentina
[c] Instituto de Investigaciones en Fisicoquímica de Córdoba (INFIQC)-CONICET, Departamento de Fisicoquímica, Facultad de Ciencias Químicas, Universidad Nacional de Córdoba, Ciudad Universitaria, X5000HUA Córdoba, Argentina

ARTICLE INFO

Article history:
Received 17 May 2011
Received in revised form 26 July 2011
Accepted 26 July 2011
Available online 4 August 2011

Keywords:
Hexacyanoferrate (III)
Powder X-ray diffraction
Rietveld analysis
Infrared spectroscopy
Thermal analysis

ABSTRACT

$Y[Fe(CN)_6]\cdot 4H_2O$ has been synthesized and characterized. The crystal structure was refined by Rietveld analysis using X-ray powder diffraction data. $Y[Fe(CN)_6]\cdot 4H_2O$ crystallizes in the orthorhombic crystal system, space group *Cmcm*. Y^{3+} ion is eight-coordinated forming a bicapped distorted trigonal prism YN_6O_2. Fe^{3+} ion is six-coordinated in the form of an irregular octahedra FeC_6 group and cyanide linkages between YN_6O_2 and FeC_6 groups build an infinite polymeric array. The vibrational spectrum shows two bands corresponding to antisymmetric and symmetric stretching $^{12}C^{14}N$ in the CN stretching region. These bands are accompanied by four weak isotopic bands at lower frequency due to the presence of ^{13}C and ^{15}N in relative natural abundance. The HOH bending band split into three bands around 1600 cm^{-1} due to the presence of two kinds of water molecules in the structure. The thermal decomposition has been followed by thermogravimetric and differential thermal analysis, IR spectroscopy and powder XRD. The size and morphology of the complex and its thermal decomposition products were evaluated by scanning electron microscopy. The magnetic measurements confirm that $Y[Fe(CN)_6]\cdot 4H_2O$ shows an antiferromagnetic order at low temperatures.

1. Introduction

The series of bimetallic coordination compounds $Ln[M(CN)_6]\cdot nH_2O$ (Ln = lanthanide; M = transition metal; $n = 4, 5$) have been the subject of numerous studies because they are important precursors for the synthesis of perovskite-type oxides which have a variety of applications such as chemical sensors and catalysts [1–4].

In hexacyanometallates the metal centers are usually found bridged by CN groups where the end C and N remain linked only to one metal. The metal linked at the C end is always with octahedral coordination to form the anionic hexacyanometallate octahedral block, $[M^n(CN)_6]^{6-n}$. The 3D framework is formed when neighboring blocks are linked at their N end through a second metal, in this case a rare-earth metal. The CN ligand has the ability to serve as bridge group between neighboring metal centers, removing electron density from the metal linked at the C end, through a π back-bonding interaction, to increase the charge density on the end N, that is the coordination site for the other metal. This leads to the overlapping between the electron clouds of neighboring metal centers and to their spin coupling and, thereby, a magnetic ordering is established. This supports the role of hexacyanometallates as prototype of molecular magnets [5–7].

Depending on the number of water molecules, these compounds crystallize in two related crystal structures: in the hexagonal structure, $P6_3/m$, or orthorhombic, *Cmcm*. The hexagonal crystal structure was confirmed for $Ln[Fe(CN)_6]\cdot 5H_2O$ with (Ln = La, Nd, Pr) [8–10] and orthorhombic crystal structure was determined on $Ln[Fe(CN)_6]\cdot 4H_2O$ (Ln = La, Nd, Pr, Sm) [11–14].

The yttrium atom has a large size, high coordination number and shows similarity in chemical behavior with the heavier lanthanide (III) ions. The structural chemistry is also similar in many ways. Cyano-bridged heterometallic Fe–Y complexes are not well documented. Recently, Kumar Karan et al. have reported a cyano-bridged polymeric complex $\{[Y(phen)_2(H_2O)_2Fe(CN)_6]\cdot 8H_2O\}_n$ where the Y^{3+} ion shows similarities in the coordination with lanthanide ions in complexes of the type $Ln[Fe(CN)_6]\cdot 4H_2O$ [15].

In the present article we report the synthesis, structural, spectroscopic and magnetic characterization of $Y[Fe(CN)_6]\cdot 4H_2O$. The crystal structure refinement of $Y[Fe(CN)_6]\cdot 4H_2O$ was performed by means Rietveld analysis using conventional X-ray powder diffraction (PXRD). These measurements were complemented by

* Corresponding author. Tel.: +54 381 4247752x7069.
E-mail address: mgomez@fbqf.unt.edu.ar (M. I. Gómez).
[1] Member of the Research Career of CONICET.

0022-2860/$ - see front matter © 2011 Elsevier B.V. All rights reserved.
doi:10.1016/j.molstruc.2011.07.051

thermogravimetric and differential thermal analysis and infrared (IR) spectroscopy. The magnetic properties of $Y[Fe(CN)_6]\cdot 4H_2O$ have been investigated.

2. Experimental

2.1. Synthesis

The bimetallic complex $Y[Fe(CN)_6]\cdot 4H_2O$ was synthesized by mixing aqueous solutions of equimolar amounts of $K_3[Fe(CN)_6]$ and $Y(NO_3)_3\cdot 6H_2O$ (prepared from the evaporation of a solution of concentrated HNO_3 and Y_2O_3) under continuous stirring at 60 °C for 2 h. The resulting orange precipitate was separated by filtration, washed with water and ethanol, and finally stored in the dark in a dry box with silica gel [16].

2.2. Characterization

Thermogravimetry (TG) and differential thermal analysis (DTA) curves were performed in a Shimadzu TGA/DTA-50 in the temperature range from 20 to 800 °C at a heating rate of 5°/min under flowing air.

Infrared spectra (in the region of 4000–400 cm^{-1}) were recorded at room temperature (RT) on a FTIR Perkin Elmer 1600 spectrophotometer in the transmission mode using KBr pellets.

PXRD profiles were obtained at RT in an X-Pert Pro PANalyticals diffractometer with Cu Kα radiation $\lambda = 1.5418$ Å, between 5° and 120° in 2θ in steps of 0.02° and step time of 10 s. The crystal structure refinement was performed by means of the Rietveld method [17] using the FULLPROF program [18] in the space group *Cmcm* using as initial model the structure of $Er[Fe(CN)_6]\cdot 4H_2O$ [19]. A pseudo-Voigt function convoluted with an axial divergence asymmetry function [20] was chosen to generate the peak shapes. The background intensities were subtracted as the linear interpolation between 26 given points. One region was excluded. The following parameters were refined: zero-point, scale factor, pseudo-Voigt parameters of the peak shape, full-width at half-maximum, atomic positions and cell parameters.

The magnetic measurements in the temperature range 5–300 K were performed with a Quantum Design superconducting quantum interference device (SQUID). The Magnetization values were measured under zero field-cooled (ZFC) and field-cooled (FC) conditions at an applied magnetic field of 5 T.

The size and morphology of the particles were determined by scanning electron microscopy (SEM) in a ZEIS SUPRA-55 VP microscope and the chemical composition of the powder was determined by energy dispersive spectroscopy (EDS) with an Oxford INCA PentaFet X3 energy dispersive X-ray analyzer.

3. Results and discussion

3.1. Crystal structure refinement

The powder XRD of $Y[Fe(CN)_6]\cdot 4H_2O$ refined at RT is shown in Fig. 1. No impurities were observed in the pattern. Final cell parameters, atomic positions and discrepancy parameters are shown in Table 1. Some selected interatomic distances and angles are shown in Table 2.

In the crystal structure of tetrahydrate $Y[Fe(CN)_6]\cdot 4H_2O$, Y^{3+} ions are eight coordinated to four N(1), two N(2) and two O(1) forming a bicapped distorted trigonal prism (YN_6O_2). This type of geometry is very common for many yttrium and lanthanide complexes. Y^{3+} is located in the Wyckoff site 4c of the space group *Cmcm* with a site symmetry *m2m*, consistent with the square antiprism 8-fold coordination. Fe^{3+} is coordinated to four C(1) and two C(2) with the usual irregular octahedral coordination (FeC_6). Bicapped trigonal prisms YN_6O_2 and irregular octahedra FeC_6 are bridged through cyano groups (see Fig. 2). There are two uncoordinated water molecules occupying zeolitic holes in the structure. The two O(2) are hydrogen bonded to the coordinated water molecules.

The Fe—C and C—N distances lie in the narrow ranges, 1.868(9)–1.950(1) and 1.022(2)–1.144(1) Å, respectively; the C—Fe—C angles for the cis positions vary from 86.2(7)° to 93.8(8)°. The CN groups are bonded linearly to Fe as shown by the values 165.6(9)–166.7(8)° for the Fe—C—N angles. Similarly, the Y—N—C bridge angles, 170.5(3)°, are also close to linear suggesting a very favorable position for relatively strong Y—NC—Fe bonding. The Y—O distance 2.580(5) Å in this compound is longer than $Y—OH_2$ 2.386 Å for another yttrium complex like $[Y(H_2O)_6(OSMe_2)_2]Cl_3$ [21].

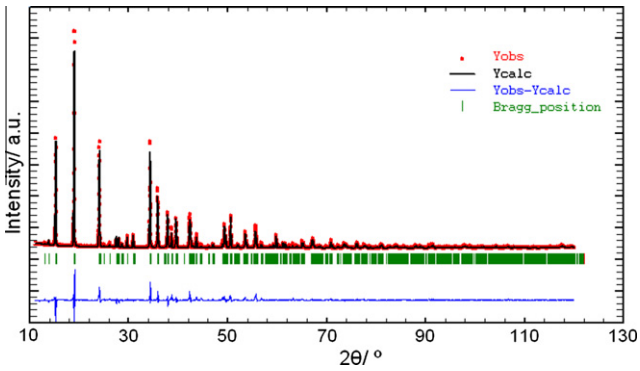

Fig. 1. Rietveld analysis of PXRD data for $Y[Fe(CN)_6]\cdot 4H_2O$.

Table 1
Crystallographic parameters for $Y[Fe(CN)_6]\cdot 4H_2O$ after Rietveld refinement with PXRD data obtained at RT.

Atom	Wyckoff site	*x*	*y*	*z*
Y	4c	0	0.3243(2)	0.25
Fe	4a	0	0	0
C1	16h	0.3185(1)	0.4509(1)	0.0939(8)
C2	8f	0	0.1297(7)	0.0633(7)
N1	16h	0.2028(5)	0.4320(4)	0.1316(4)
N2	8f	0	0.2169(6)	0.0819(5)
O1	8g	0.2874(6)	0.2082(4)	0.25
O2	8f	0	0.6568(4)	0.1049(3)

Space group: *Cmcm*; cell parameters: $a = 7.342(1)$ Å, $b = 12.788(1)$ Å, $c = 13{,}603(1)$ Å. Vol = 1277.31(2) $Å^3$, $Z = 4$.
Discrepancy factors: $R_{wp} = 21.3$, $R_{exp} = 4.23$, $R_p = 17.4$, $R_{Bragg} = 11.1$.

Table 2
Some selected interatomic distances (Å) and angles (°) in $Y[Fe(CN)_6]\cdot 4H_2O$.

Interatomic distances (Å)		Bond angles (°)	
Y—N		(N1)—(Y)—(N1)	115.7(3)
(Y)—(N1)	2.589(5) × 4	(N2)—(Y)—(N2)	118.0(4)
(Y)—(N2)	2.668(7) × 2	(N1)—(Y)—(N2)	75.0(3)
		(N1)—(Y)—(N2)	143.8(4)
Y—O		(O1)—(Y)—(O1)	109.7(3)
(Y)—(O1)	2.580(5)	(O1)—(Y)—(N1)	80.5(2)
		(O1)—(Y)—(N1)	140.9(3)
Fe—C		(O1)—(Y)—(N2)	72.8(2)
(Fe)—(C1)	1.950(1) × 4	(C1)—(Fe)—(C1)	86.2(7)
(Fe)—(C2)	1.868(9) × 2	(C1)—(Fe)—(C1)	180.0(1)
C—N		(C1)—(Fe)—(C1)	93.8(8)
(C1)—(N1)	1.022(2) × 2	(C1)—(Fe)—(C2)	89.1(8)
(C2)—(N2)	1.144(1) × 2	(C1)—(Fe)—(C2)	90.9(7)
(O1)···(O2)	2.601(4)	(C2)—(Fe)—(C2)	180.0(9)

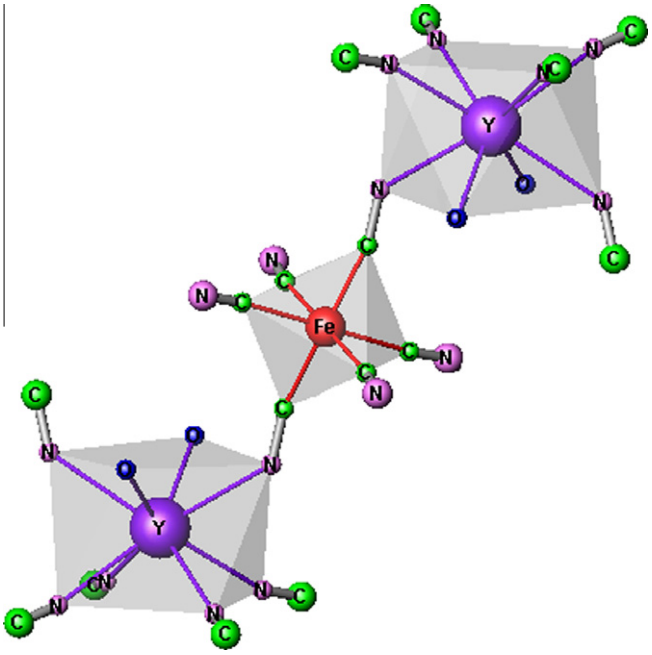

Fig. 2. View of the structure of $Y[Fe(CN)_6]\cdot 4H_2O$ showing coordination around Y and Fe.

Zhou et al. prepared $[FeY(CN)_6(C_6H_{11}NO)_2(H_2O)_4]$ using caprolactam as a ligand. In this complex Y^{3+} is seven coordinated and has approximately pentagonal-bipyramidal stereochemistry, with water molecules occupying apical positions [22].

This crystal structure is in agreement with those previously published for $Ln[Fe(CN)_6]\cdot 4H_2O$, *Ln* = Nd [12], Er [19], Pr [10], Sm [23] and Gd [24]. Hulliger et al. have demonstrated a linear relationship between cell parameters and the ionic radius of the rare-earth element for the lanthanide ferri- and chromi-cyanides [25]. Fig. 3 shows the linear increase of cell parameters of lanthanide ferricyanides with the ionic radius of lanthanides [25]. The yttrium ion has a large size (1.02 Å) and shows similarity in chemical and structural behavior with the lanthanide (III) ions. According to the results discussed previously, the lighter lanthanide metals such as La, Pr and Nd formed pentahydrates, and the other heavier metals (Ln = Sm—Lu) led tetrahydrates.

In pentahydrates $Ln[Fe(CN)_6]\cdot 5H_2O$, *Ln* = Nd, Pr or La, Ln^{3+} ion is nine-coordinated in the form of LnN_6O_3 group forming a tricapped trigonal prism. Fe^{3+} is six-coordinated in the form of an octahedral FeC_6 group and cyanide linkages between LnN_6O_3 and FeC_6 groups

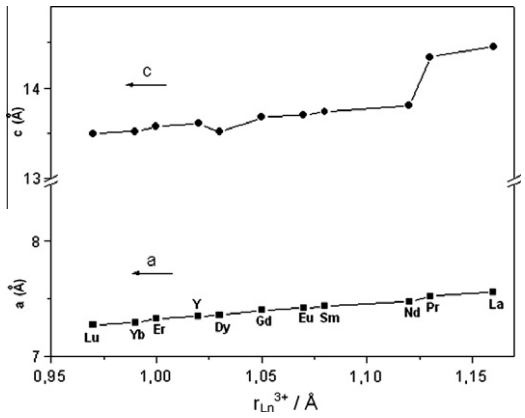

Fig. 3. Variation of cell parameters of lanthanide ferricyanides with the ionic radius.

build an infinite polymeric array. Pentahydrate complexes formed by La and Nd are very unstable and convert to the stable tetrahydrate by losing one water molecule [8,9]. In our case we have not observed the formation of pentahydrate $Y[Fe(CN)_6]\cdot 5H_2O$ indicating that the tetrahydrate is very stable due to the fact that Y^{3+} has the correct size for an 8-fold coordination.

3.2. Fourier transform infrared spectroscopy (FTIR)

Fig. 4a shows the complete FTIR spectrum of $Y[Fe(CN)_6]\cdot 4H_2O$ at room temperature in KBr disks. The analysis of the results confirms the structural data determined by PXRD measurements.

3.2.1. C≡N stretching bands

Fig. 4b shows the IR spectrum in the CN stretching region. The strong bands marked **a** (at 2152 cm^{-1}) and **b** (at 2142 cm^{-1}) in Fig. 4b, are $^{12}C^{14}N$ stretching bands of the bridged Y—N≡C—Fe system and corresponds to the antisymmetric and symmetric ν(CN) stretching. The very weak bands marked **c** (at 2124 cm^{-1}) and **d** (at 2116 cm^{-1}) are $^{12}C^{15}N$ stretching bands, whereas those labeled **e** (at 2110 cm^{-1}) and **f** (at 2100 cm^{-1}) are $^{13}C^{14}N$ stretching bands. The broad band labeled **g**, with maximum intensity at 2070 cm^{-1} could be a difference band or a combination band due to the prominent water bending modes and the Fe—C stretch [26].

3.2.2. Water bands

The presence of two kinds of crystallographically inequivalent water molecules in the lattice is evidenced by their IR characteristic vibrational modes. The frequency values are lower than those expected for free water stretching vibrations. This fact agrees not only with water coordination of the Y(III) ion but also with the presence of hydrogen bonds in the lattice [27].

In Fig. 4a, the highest frequency band in the δ(HOH) region, at 1680 cm^{-1}, is attributed to those water molecules with the strong interaction with Y^{3+}, the intermediate one at 1640 cm^{-1} belongs to coordinated water molecules but with a weaker coordination bond and the band at 1610 cm^{-1} corresponds to the weakly bonded water. The two narrow bands at 3612 and 3536 cm^{-1} can be

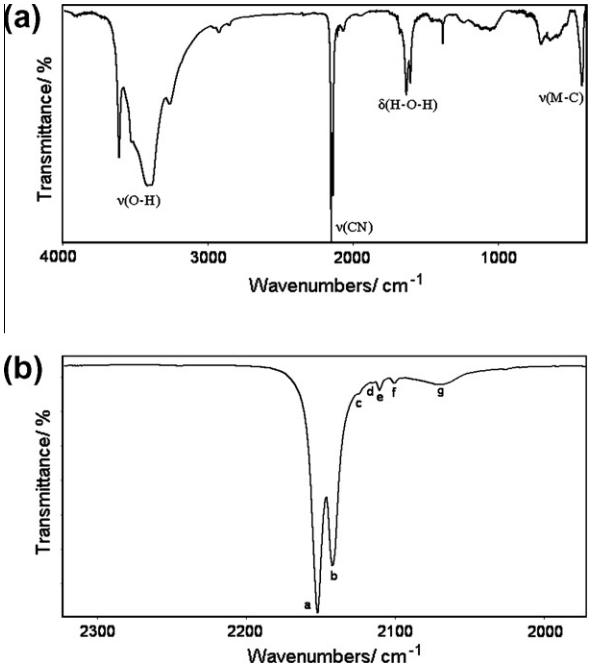

Fig. 4. (a) IR spectra of $Y[Fe(CN)_6]\cdot 4H_2O$ in the 4000–400 cm^{-1} range and (b) IR spectra of $Y[Fe(CN)_6]\cdot 4H_2O$ between 2350 and 2000 cm^{-1}.

assigned to the stretching O—H of coordinated water. The broad stretching bands in the region of 3450–3260 cm^{-1} are due to zeolitic water.

The librational modes of coordinated water, which usually present low intensity and are overlapped with other modes, are difficult to identify. The bands at 810, 710, 532 and 410 cm^{-1} can be assigned to water modes. The two bands at the highest frequencies correspond to the rocking motion, whereas the band at 532 cm^{-1} is associated to wagging and twisting modes and the band at 410 cm^{-1} is attributed to M—OH_2 stretching vibration [28].

3.2.3. M—C≡N and M—C bands

The δ(M—C≡N) and ν(M—C) vibrations are observed at 595 and 430 cm^{-1} respectively. These values are observed in the expected frequency values for hexacyanometallates (III) [27].

3.3. Thermal decomposition of $Y[Fe(CN)_6]\cdot 4H_2O$

TG and DTA data for $Y[Fe(CN)_6]\cdot 4H_2O$ are shown in Fig. 5. Three main steps are observed in TGA for the decomposition process in air. The first one ends at 175 °C, with a mass loss of 14.94% due to the loss of three water molecules (theoretical value 14.49%). The second one finishes at 265 °C and corresponds to the loss of the remaining water molecule to obtain the anhydrous complex. DTA curve shows two endothermic peaks at 142 and 187 °C, both due to dehydration. This suggests the existence of two types of water molecules in the crystal structure and it is in agreement with IR spectroscopy data and the results of the refinement of the crystal structure. The third step in TGA, which finishes at 650 °C, has a mass loss of 28.42%. This mass loss was attributed to the elimination and oxidation of the cyanide groups with the simultaneous formation of simple oxides (Y_2O_3, Fe_2O_3) and a perovskite compound $YFeO_3$ with hexagonal structure. A very exothermic peak is observed in DTA at 359 °C.

At temperatures higher than 650 °C the mass remained constant and the simple oxides react to produce $YFeO_3$.

The total mass loss from room temperature to 650 °C is 48.11%. This is in agreement with the theoretical mass loss (48.28%) calculated for the formation of $YFeO_3$ as final product from the complex [16].

3.4. Magnetic properties

Fig. 6a shows the temperature dependence of the magnetization under both ZFC (zero field cooling) and FC (field cooling) conditions for $Y[Fe(CN)_6]\cdot 4H_2O$. No difference between both curves is observed, indicating the absence of any long range magnetic ordering.

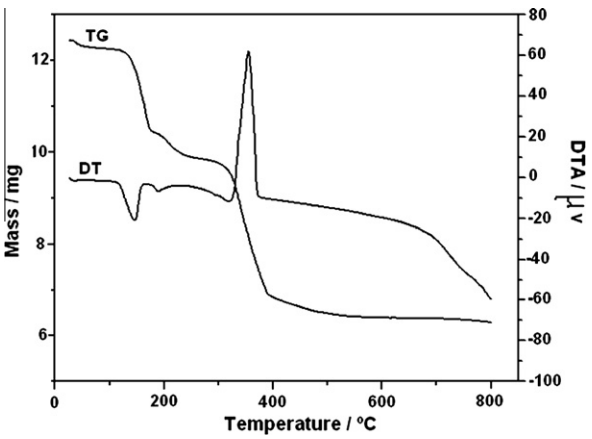

Fig. 5. TGA and DTA curves for $Y[Fe(CN)_6]\cdot 4H_2O$ in air.

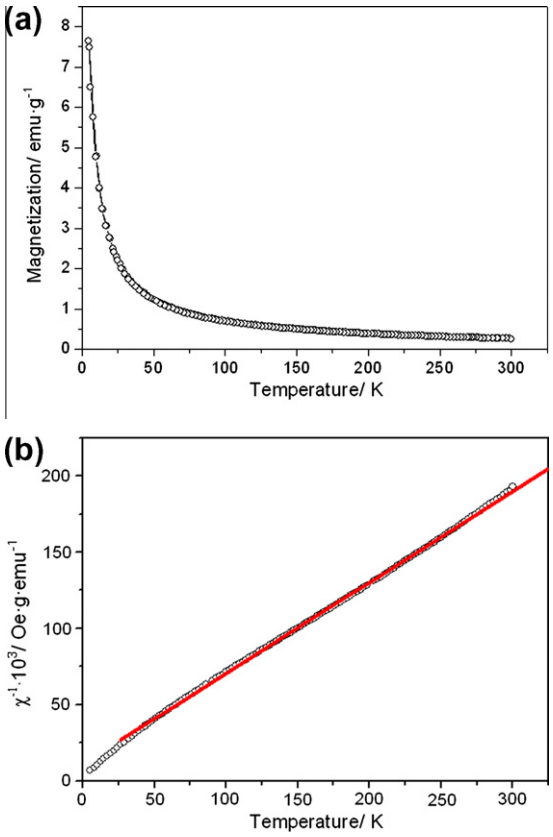

Fig. 6. (a) Field cooled (FC) and zero field cooled (ZFC) magnetization curves at 5 T for $Y[Fe(CN)_6]\cdot 4H_2O$ and (b) temperature dependence of χ^{-1} curves of $Y[Fe(CN)_6]\cdot 4H_2O$.

Fig. 6b shows temperature dependence of χ^{-1} in the temperature range 5–300 K.

The magnetic behavior of $Y[Fe(CN)_6]\cdot 4H_2O$ is similar to that ordinary transition elements compounds obeying a Curie–Weiss law. Straight line is the fit to the curve in the temperature range 50–300 K. The Curie constant, C, and the Curie–Weiss temperature, θ, are determined from a linear fitting of $(1/\chi) = (T-\theta)/C$ (Curie–Weiss law) in the linear region. Fitting yielded $C = 1.60 \times 10^{-3}$ emu K/(g Oe) and $\theta = -6.36$ K. The negative value of θ indicates the presence of antiferromagnetic interactions. The obtained effective magnetic moment ($\mu_{eff} = 2.185\ \mu_B$) is a little higher than the value $\mu_{eff} = 1.73\ \mu_B$ expected for Fe^{3+} in the low spin state. This value is very similar to the reported value ($\mu_{eff} = 2.18\ \mu_B$) for $La[Fe(CN)_6]\cdot 5H_2O$ by Mitróova et al. [29]. From the spectrochemical series we find that CN ligand usually create a strong ligand field and the $[Fe(CN)_6]^{3-}$ complex exhibits a magnetic moment equal to 1.73 μ_B. This means that the Fe^{3+} (d^5) ion, the only paramagnetic ion in the complex, contains one unpaired electron, and hence it is in the low-spin configuration (t_{2g}^5), $S = 1/2$. The unsymmetric filling of the orbital triplet can lead to a small orbital contribution to the magnetic moment [30].

Yttrium ferricyanide tetrahydrate is an example of anti-ferromagnetic behavior because in this complex, the superexchange is established through the overlapping of identical t_{2g}^5 orbitals from iron atoms, and its antiferromagnetic nature is a result of the Pauli Exclusion Principle [31].

3.5. Scanning electron microscopy (SEM)

The size and morphologies of $Y[Fe(CN)_6]\cdot 4H_2O$ and its thermal decomposition products were investigated by SEM as shown in

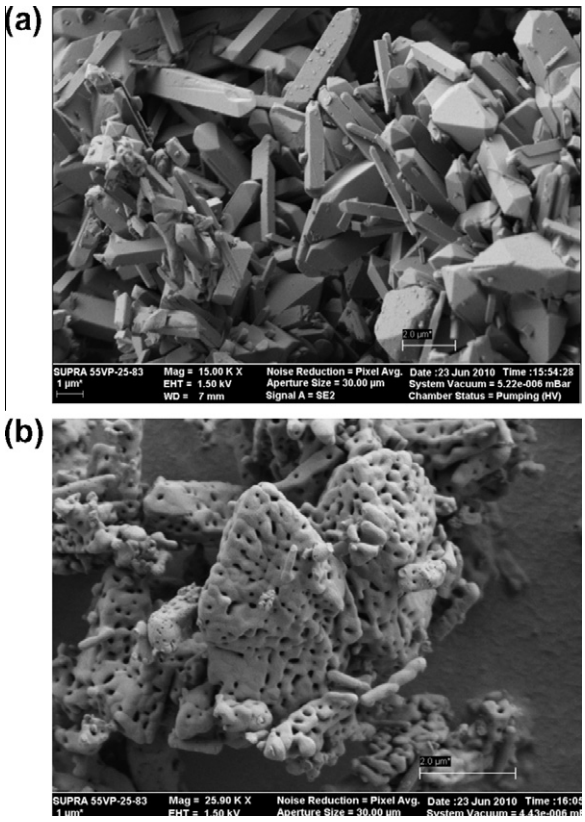

Fig. 7. Scanning electron microscopy of (a) $Y[Fe(CN)_6]\cdot 4H_2O$ and (b) orthorhombic $YFeO_3$.

Fig. 7. The SEM photograph of $Y[Fe(CN)_6]\cdot 4H_2O$ (Fig. 7a) powder shows that is composed of well defined large crystals with different shapes and with sharp edges up to 3 μm in size. The SEM photograph of orthorhombic $YFeO_3$ obtained at temperatures higher than 800 °C (Fig. 7b) clearly shows that the shape and morphology is quite different to that of the complex. The large crystals of the complex were completely disrupted and the sponge-like and porous agglomerate with pore size of about 0.1 μm appeared. The pores are formed by fast expulsion of gas evolving during the decomposition process.

4. Conclusions

$Y[Fe(CN)_6]\cdot 4H_2O$ crystallizes in the orthorhombic crystal system, space group *Cmcm*, cell parameters $a = 7.342(1)$ Å, $b = 12.788(1)$ Å, $c = 13{,}603(1)$ Å. In this structure the Y^{3+} ion is eight-coordinated in the form of a $Y(N_6O_2)$ group; the Fe^{3+} ion is six-coordinated in the form of an octahedral FeC_6 group; and cyanide linkages between $Y(N_6O_2)$ and FeC_6 groups build an infinite polymeric array. Two uncoordinated water molecules occupy zeolitic holes.

$Y[Fe(CN)_6]\cdot 4H_2O$ decomposes in four steps. The first one corresponds to the elimination of three water molecules loosely bonded (non-coordinated water), the second one to the loss of the remaining water molecule strongly bounded (coordinated water), the third one to the cyanide elimination to give hexagonal $YFeO_3$ mixed with Fe_2O_3 and Y_2O_3, and finally in the fourth step (without mass loss) well crystallized orthorhombic $YFeO_3$ was formed as a final product.

The values $\mu_{eff} = 2.185\ \mu_B$, and Curie–Weiss temperature, $\theta = -6.36$ K, were determined from the Curie–Weiss law. The negative value of θ indicates the presence of antiferromagnetic interactions in the complex at low temperatures.

The complex is composed of well defined large crystals with different shapes and with sharp edges up to 3 μm in size. Orthorhombic $YFeO_3$ obtained at temperatures higher than 650 °C is a sponge-like and porous agglomerate with pore size of about 0.1 μm.

Acknowledgments

R.E.C. thanks ANPCYT for PICT2007 303, CONICET for PIP #11220090100995 and SECyT-UNC for Project 159/09. D.M.G. thanks CONICET for a fellowship. D.M.G., M.C.N. and M.I.G. thank CIUNT for financial support.

References

[1] L. Wu, J. Yu, L. Zhang, X. Wang, S. Li, J. Solid State Chem. 177 (2004) 3666–3674.
[2] X. Lu, J. Xie, H. Shu, J. Liu, C. Yin, J. Lin, Mater. Sci. Eng. B 138 (2007) 289–292.
[3] J. Lentmaier, S. Kemmler-Sack, G. Knell, P. Kessler, P. Plies, Mater. Res. Bull. 31 (1996) 1269–1276.
[4] J. Lentmaier, S. Kemmler-Sack, Mater. Res. Bull. 33 (1998) 461–473.
[5] M. Avila, L. Reguera, J. Rodriguez-Hernandez, J. Balmaseda, E. Reguera, J. Solid State Chem. 181 (2008) 2899–2907.
[6] J. Rodriguez-Hernandez, A. Gomez, E. Reguera, J. Phys. D: Appl. Phys. 40 (2007) 6076–60872.
[7] R. Martinez Garcia, L. Reguera, M. Knobel, E. Reguera, J. Phys.: Condens. Matter 19 (2007) 1–11.
[8] W.E. Bailey, R.J. Williams, W.O. Milligan, Acta Crystallogr. B 29 (1973) 1365.
[9] W. Xiaoyu, Y. Yukawa, Y. Masuda, J. Alloys Compd. 290 (1999) 85–90.
[10] L. Zhang, X. Zhou, T. Mak, P. Tanner, Polyhedron 26 (2007) 4019–4023.
[11] D.F. Mullica, W.O. Milligan, L.R. Garner, Acta Crystallogr. B 36 (1980) 2561–2564.
[12] M.C. Navarro, E.V. Pannunzio-Miner, S. Pagola, M.I. Gómez, R.E. Carbonio, J. Solid State Chem. 178 (2005) 847–854.
[13] V. Kavekansky, J. Kovac, M. Zentrova, I. Zezula, Czech. J. Phys. 52 (2002) 333–336.
[14] W. Petter, V. Gramlich, F. Hulliger, J. Solid State Chem. 74 (1988) 9.
[15] N. Kumar Karan, S. Mitra, G.M. Golzar Hossain, K.M. Abdul Malik, Z. Naturforsch. 57b (2002) 736–740.
[16] D.M. Gil, M.C. Navarro, M.C. Lagarrigue, J. Guimpel, R.E. Carbonio, M.I. Gómez, J. Therm. Anal. Calorim. 103 (3) (2011) 889–896.
[17] R.A. Young, The Rietveld Method, Oxford Scientific Publications, UK, 1995.
[18] J. Rodriguez-Carbajal, Physica B 192 (1993) 55–69.
[19] A. Dommann, H. Vetsch, F. Hulliguer, Acta Crystallogr. C 46 (1990) 1992–1994.
[20] L.W. Finger, D.E. Cox, A.P. Jephcoat, J. Appl. Crystallogr. 27 (1994) 892–900.
[21] O. Kristiansson, Lindqvist-Reis, Acta Crystallogr. C 56 (2000) 163–164.
[22] B.C. Zhou, H. Kou, Y. He, M. Xiong, R.J. Wang, Y. Li, Acta Crystallogr. C 58 (2002) 478–480.
[23] D. Mullica, E. Sappenfield, J. Solid State Chem. 82 (1989) 168–171.
[24] D.F. Mullica, E.L. Sappenfield, Acta Crystallogr. C 47 (1991) 2433–2435.
[25] F. Hulliger, M. Landolt, H. Vetsch, J. Solid State Chem. 18 (1976) 283–291.
[26] X. Zhou, W. Wong, M. Faucher, P. Tanner, J. Solid State Chem. 181 (2008) 3057–3064.
[27] K. Nakamoto, Infrared and Raman Spectra of Inorganic and Coordination Compounds, Wiley, New York, 1986.
[28] V.P. Mahadevan Pillai, V.U. Nayar, V.B. Jordanovska, J. Solid State Chem. 133 (1997) 407–415.
[29] Z. Mitróova, M. Mihalik, A. Zento, M. Lukácová, Czech. J. Phys. 54 (2004) 559–562.
[30] S. Juszczyk, C. Johansson, M. Hanson, A. Ratusznna, G. Matecki, J. Phys.: Condens. Matter 6 (1994) 5697–5706.
[31] R. Martinez-García, M. Knobel, E. Reguera, J. Phys. Chem. B 110 (2006) 7296–7303.